S1 Supplementary Results: Why are biting flies attracted to blue objects?

A. Sensitivity of findings to assumptions

In our manuscript we calculate photoreceptor quantum catches (*Q*) using photoreceptor sensitivity curves established for *Musca* and *Calliphora*. Because photoreceptor excitation relates non-linearly to the number of quanta absorbed, we calculate *E* through the transformation of *Q* as follows:

$$E = \ln(Q)$$

To demonstrate that our findings are not se.nsitive to assumptions made in these calculations, we repeated our analyses using three variations on these procedures. In the first of these, we provided *Q* values directly as input to ANNs without non-linearisation. In the second, we calculated *E′* as input to ANNs as follows (after [1]):

$$E' = \frac{Q}{Q+1}$$

In the third, we calculated *E* values using photoreceptor sensitivity curves recorded for tsetse (see fig S1) [2, 3], henceforth referred to as E^t. Results are shown in figs S2-S4, and tables S1-S3. In each case, findings are equivalent to those presented in our manuscript. In figure S4, R1-6 and R8y effects are consistently evident, but patterns for other receptors are variable, as discussed in our manuscript.

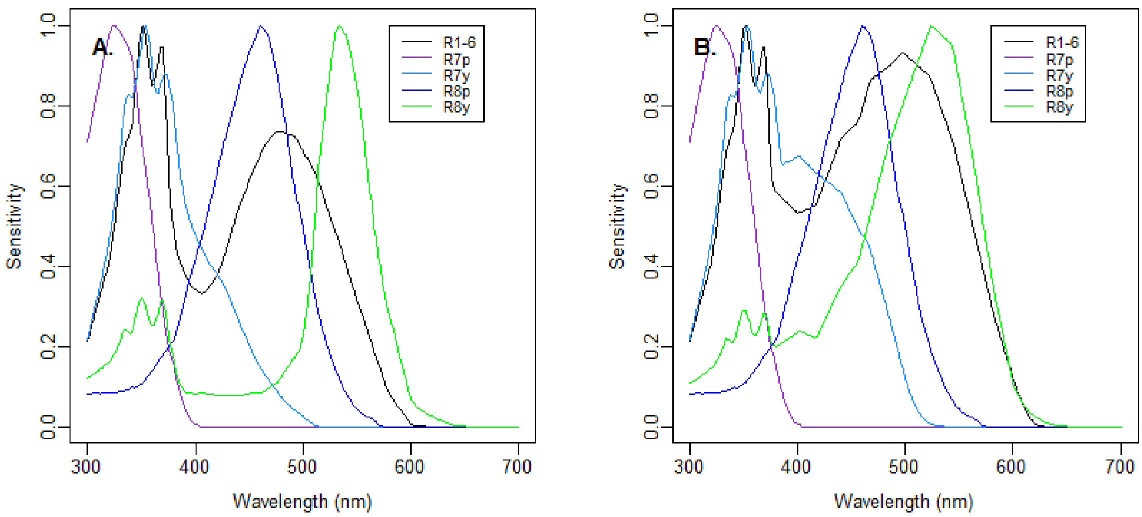

Figure S1. Photoreceptor sensitivity curves for *Musca* and *Calliphora* (A), and for *Glossina morsitans* (B). Curves in A are as presented in our manuscript, those in B were created by [3] based on original recordings by [2]

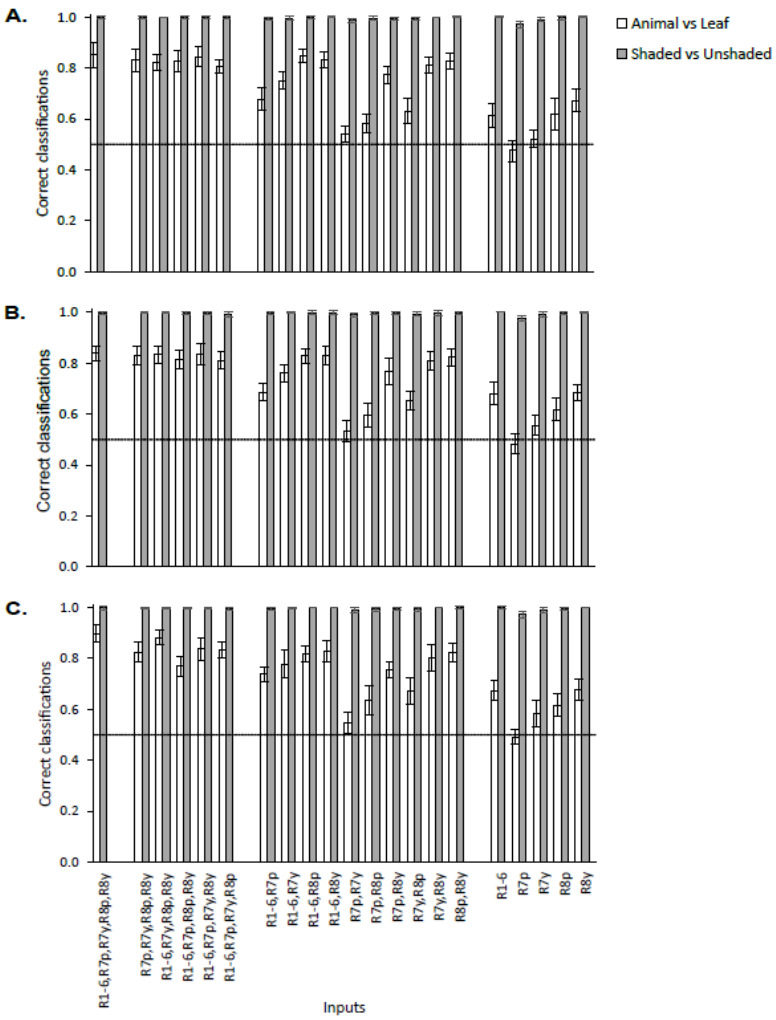

Figure S2. The accuracy of trained ANNs in classifying a set of test stimuli not experienced during training, according to the number of photoreceptor excitation inputs they received. (A) *Q* values as inputs, (B) *E′* values as inputs, (C) E^t values as inputs. Results are equivalent for each case. Animal-ANNs with more photoreceptor inputs had greater classification accuracy, but shaded-ANNs were equally accurate regardless of their number of photoreceptor inputs. Each plot presents results for the best 20 ANNs of each type, collated as means and sample standard deviations.

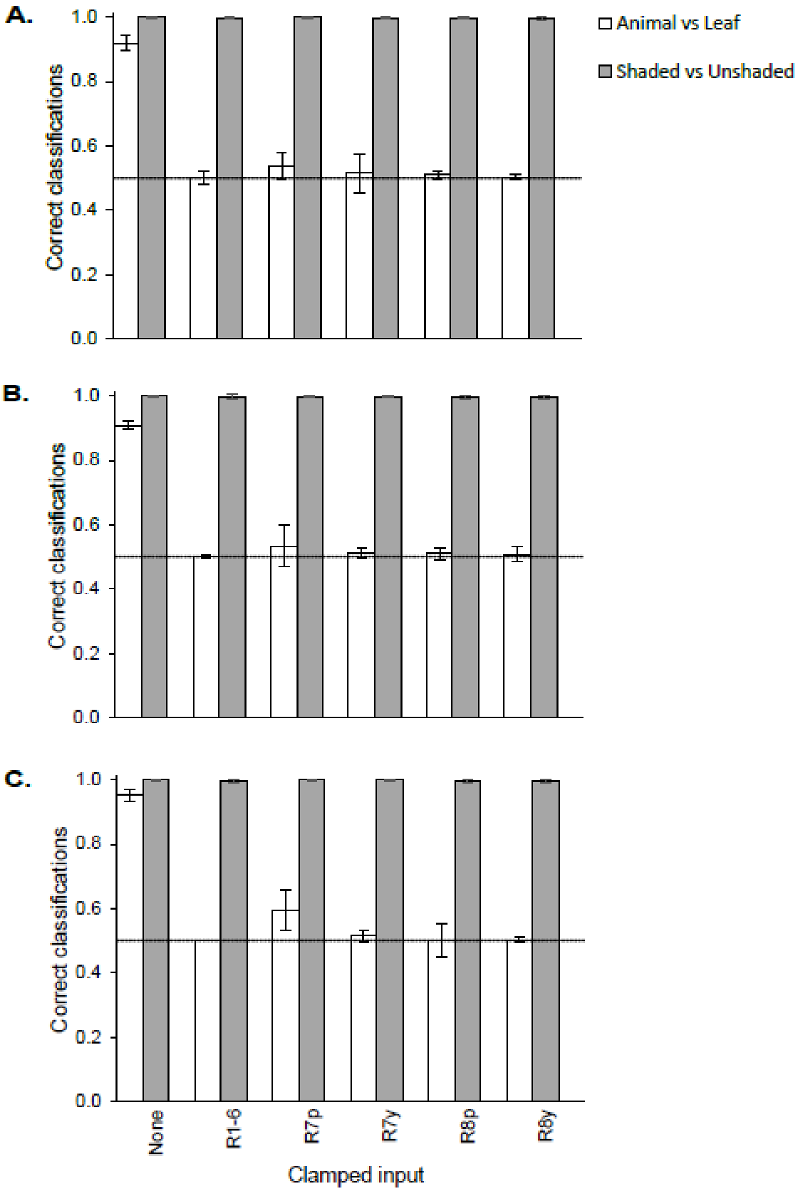

Figure S3. Evaluation of ANNs trained to distinguish 'animal' and 'shaded' stimuli. The accuracy of trained ANNs in classifying the complete dataset of stimuli with the excitation value of individual photoreceptor excitation inputs clamped to their median values. Data are for the full ANNs receiving all five photoreceptor inputs. (A) *Q* values as inputs, (B) *E'* values as inputs, (C) E^t values as inputs. Results are equivalent for each case. Clamping any photoreceptor excitation value reduced the accuracy of animal-ANNs to random chance, indicating that all were important to accurate classification. However, clamping had no effect on the classification accuracy of shaded-ANNs, demonstrating that no single photoreceptor input was critical to that process. Each plot presents results for the best 20 ANNs of each type, collated as means and sample standard deviations.

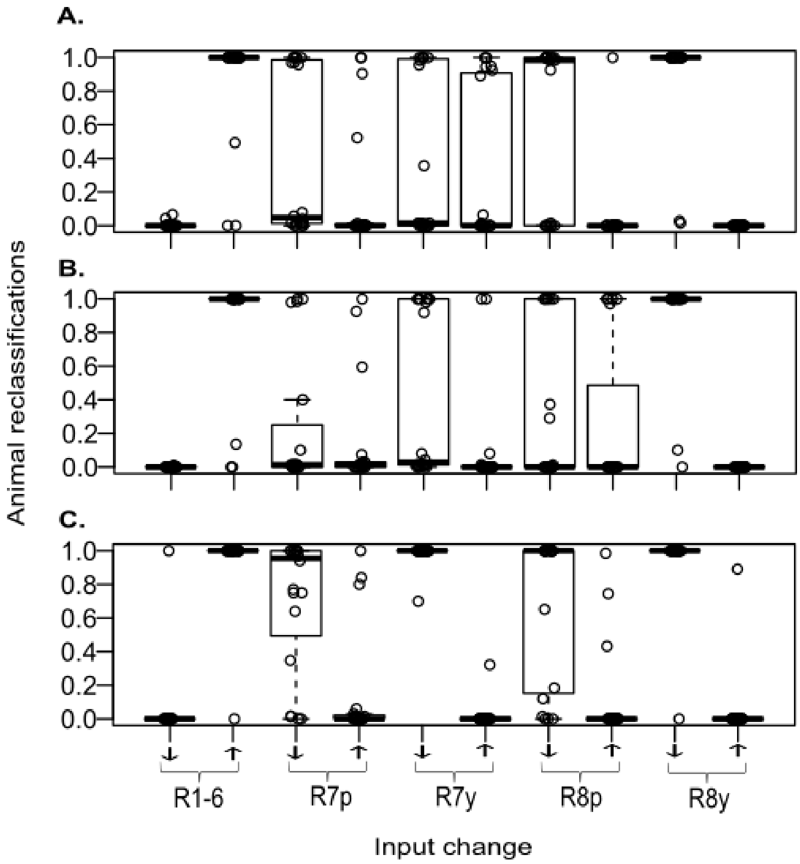

Figure S4. The contribution of photoreceptor excitation signals to 'animal' classifications. (A) *Q* values as inputs, (B) *E'* values as inputs, (C) E^t values as inputs. Plots consider only those stimuli whose classification changed as a result of clamping in fig S3. The proportion of these reclassifications in which the classification changed from 'leaf' to 'animal' is shown, according to whether clamping increased or decreased the relevant photoreceptor excitation value for a given stimulus (indicated by an arrow). Increases in the excitation of blue-sensitive R1-6 are associated with stimuli being reclassified as 'animal', and decreases are associated with reclassification as 'leaf'. Increases in the excitation of green-sensitive R8y are associated with stimuli being reclassified as 'leaf', and decreases are associated with reclassification as 'animal'. Trends for other photoreceptors are somewhat variable according to the way that excitation inputs were calculated, as discussed in our manuscript. Each plot presents results for the best 20 ANNs of each type. Individual datapoints are plotted, superimposed over boxplots showing 25th, 50th and 75th percentiles.

Table S1. The proportion of the 20 best ANNs of each type that classified fabrics used in biting fly control as 'animal' or as 'shaded'. *Q* values as inputs.

Fabric	'Animal' classifications	'Shaded' classifications
Phthalogen blue cotton [4]	0.65 (0.75)	0.00 (1.00)
Phthalogen blue cotton [5]	0.70 (0.85)	0.00 (1.00)
Blue fabric [6]	0.65 (0.85)	0.00 (1.00)
'Phthalogen blue' polyester [4]	0.65 (0.85)	0.00 (0.90)
Royal blue polyester [4]	0.50 (0.30)	0.00 (1.00)
Typical blue polyester [7]	0.80 (0.90)	0.00 (0.55)
ZeroFly® blue polyester [7]	0.70 (0.85)	0.00 (1.00)
Black cotton [4]	0.60 (0.60)	0.00 (1.00)
Black polyester [4]	0.65 (0.65)	0.00 (1.00)
Black cotton [7]	0.95 (0.95)	0.00 (1.00)
Violet polyester [7]	0.25 (0.40)	0.00 (1.00)

Proportions are for fabrics under open/cloudy illumination, with those for woodland shade illumination in brackets.

Table S2. The proportion of the 20 best ANNs of each type that classified fabrics used in biting fly control as 'animal' or as 'shaded'. *E'* values as inputs.

Fabric	'Animal' classifications	'Shaded' classifications
Phthalogen blue cotton [4]	0.85 (0.90)	0.00 (1.00)
Phthalogen blue cotton [5]	0.55 (0.90)	0.00 (1.00)
Blue fabric [6]	0.65 (0.80)	0.00 (1.00)
'Phthalogen blue' polyester [4]	0.85 (0.85)	0.00 (0.85)
Royal blue polyester [4]	0.95 (0.60)	0.00 (1.00)
Typical blue polyester [7]	0.85 (0.85)	0.00 (0.40)
ZeroFly® blue polyester [7]	0.65 (0.85)	0.00 (1.00)
Black cotton [4]	0.90 (0.80)	0.00 (1.00)
Black polyester [4]	0.85 (0.75)	0.00 (1.00)
Black cotton [7]	0.90 (0.95)	0.00 (1.00)
Violet polyester [7]	0.75 (0.50)	0.00 (1.00)

Table S3. The proportion of the 20 best ANNs of each type that classified fabrics used in biting fly control as 'animal' or as 'shaded'. E^t values as inputs.

Fabric	'Animal' classifications	'Shaded' classifications
Phthalogen blue cotton [4]	0.80 (0.80)	0.00 (1.00)
Phthalogen blue cotton [5]	0.85 (0.85)	0.00 (1.00)
Blue fabric [6]	0.80 (0.80)	0.00 (1.00)
'Phthalogen blue' polyester [4]	0.80 (0.85)	0.00 (0.80)
Royal blue polyester [4]	0.90 (0.95)	0.00 (1.00)
Typical blue polyester [7]	0.65 (0.90)	0.00 (0.55)
ZeroFly® blue polyester [7]	0.80 (0.80)	0.00 (1.00)
Black cotton [4]	1.00 (1.00)	0.05 (1.00)
Black polyester [4]	1.00 (1.00)	0.00 (1.00)
Black cotton [7]	1.00 (1.00)	0.05 (1.00)
Violet polyester [7]	0.90 (0.95)	0.00 (1.00)

B. Additional evidence for opponent processing of photoreceptor inputs for animal classification, and use of achromatic information for shaded classification

In our manuscript we interrogate 20 trained ANNs that made ‘animal’ or ‘shaded’ classifications based on five fly photoreceptor excitation inputs. We analyse the contributions of those photoreceptor inputs to classification using the clamping method, which reveals that ANNs rely on chromatic information (i.e. photoreceptor response comparisons) for ‘animal’ classifications, and achromatic information (i.e. information in individual photoreceptor responses, or sums of photoreceptor responses) for ‘shaded’ classifications.

Additional evidence for this principle can be found in the connection weights of these trained ANNs (fig S5). In these ANNs, three hidden cells each received input from all five fly photoreceptor excitation values (fig S5A). For each hidden cell in animal-ANNs, these inputs were connected with a mix of positive and negative weights, demonstrating that the hidden cells compared the responses of subsets of photoreceptors (fig S5B). Further comparison often occurred at the level of the output cell, by virtue of connection weights from hidden cells also differing in their sign (fig S5B). Meanwhile, for each hidden cell in shaded-ANNs, the weights of the five photoreceptor inputs generally had the same sign, or else a weight with a small absolute value, indicating that hidden cells were effectively summing photoreceptor excitation signals (fig S5C). In these models, connection weights from the hidden to the output layer generally ensured that the original photoreceptor signals were summed and not compared (fig S5C).

Our analysis of the five-photoreceptor-input animal-ANNs by the clamping method suggested that green- and blue-sensitive photoreceptors were important in animal classification. Several two-photoreceptor-input models achieved similar classification accuracy (fig 2A in our manuscript), so we also interrogated the mechanisms that they used for classification. To do this, we examined all classifications of the full stimulus dataset that changed as a result of clamping a given photoreceptor signal to its median value (identical to the approach used in fig 2C of our manuscript). We divided these according to whether clamping increased or decreased the original photoreceptor signal, and examined the proportion of these reclassifications where the stimulus classification changed from ‘leaf’ to ‘animal’ (fig S6). Where these ANNs received input from a blue- (R8p, R7y, or R1-6) and green- (R8y) sensitive photoreceptor, increases in the excitation of the blue-sensitive photoreceptor tended to cause an increase in ‘animal’ classifications, and decreases in excitation tended to cause an increase in ‘leaf’ classifications. Increases in excitation of the green-sensitive photoreceptor tended to cause an increase in ‘leaf’ classifications, and decreases in excitation tended to cause an increase in ‘animal’ classifications (fig S6A-C). The remaining model received input from two blue-sensitive photoreceptors, wherein the one with peak sensitivity at longer wavelengths (R1-6) took the role played by R8y in the other models (fig S6D). Thus, the principle of operation was similar.

A.

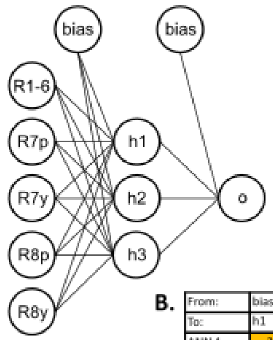

Figure S5. Connection weights for the 20 best trained ANNs, providing evidence for opponency in animal classification and achromatic information in shaded classification. (A) ANN architecture. All ANNs had an input layer of five photoreceptor signals (R1-6, R7p, R7y, R8p, R8y), a hidden layer of three cells (h1-3), and a single output cell (o). Connections between these cells are indicated by solid lines. The weights for these connections in each of the 20 best ANNs are shown in (B) and (C). Positive values >2 are coloured blue, negative values <-2 are coloured orange, lightly coloured cells indicate values close to zero. Photoreceptor inputs to each hidden cell are highlighted in bold and enclosed by thick borders. (B) In "animal" classification ANNs the photoreceptor inputs to each hidden cell comprise both positive and negative weights, indicating opponent processing. (C) In "shaded" classification ANNs, photoreceptor inputs to each hidden cell generally have weights of the same sign.

B. "Animal" classification ANNs

From:	bias	**R1-6**	**R7p**	**R7y**	**R8p**	**R8y**	bias	**R1-6**	**R7p**	**R7y**	**R8p**	**R8y**	bias	**R1-6**	**R7p**	**R7y**	**R8p**	**R8y**	bias	h1	h2	h3
To:	h1	h1	h1	h1	h1	h1	h2	h2	h2	h2	h2	h2	h3	h3	h3	h3	h3	h3	o	o	o	o
ANN 1	-3.21865	-472.662	29.47896	-2.83705	303.6817	141.1713	-18.8942	-8.68032	56.7485	-21.08	35.63244	-100.338	6.817673	266.2424	-32.0627	53.68372	-264.395	-24.3916	129.876	-214.359	84.42894	-220.105
ANN 2	-167.888	-65.8179	5.305852	36.48574	-73.3702	29.9964	3.88667	52.5777	-30.5603	67.36485	-100.37	11.98349	-6.3211	-285.711	65.21119	-111.38	273.9382	59.39	67.35076	-63.1046	-73.9632	-67.5574
ANN 3	-1.07547	76.9976	13.82105	4.031262	-66.1323	-23.9413	24.9688	-31.2631	164.2632	-92.5425	-119.659	154.5712	-22.3438	-32.7804	98.87758	-289.399	387.4973	-165.403	-98.8264	370.8919	-276.576	99.91191
ANN 4	-94.1826	-106.478	599.8699	-108.295	-272.793	-66.8904	-6.45897	-345.179	88.13712	-80.9048	213.3443	125.9221	5.759735	622.0859	179.5848	-437.847	80.49218	-435.831	-117.092	115.1864	-307.117	117.9759
ANN 5	-2.55296	-332.158	23.50935	-5.02346	211.4177	100.462	10.02124	-22.4219	-29.6313	107.2043	-160.58	104.4908	5.871566	-66.4849	53.00919	41.34053	-210.688	-62.2507	92.06418	-241.747	-247.977	150.0184
ANN 6	-4.07461	4.361632	15.86504	-39.3865	38.98665	-20.9709	9.365312	261.7569	-70.51	128.42	-270.854	-50.2834	-102.115	-47.0078	135.7132	-105.454	-106.681	63.02471	-166.905	144.7361	160.0196	-132.027
ANN 7	53.15425	92.62024	-258.92	-97.4433	229.2714	9.515184	7.716105	463.6331	-176.238	237.9212	-350.702	-175.72	-2.35226	158.3258	-221.86	630.5368	-711.294	147.6706	143.0932	-279.2	137.1018	-288.739
ANN 8	-4.93948	-411.377	243.4447	-300.888	584.1853	-96.5112	-2.73774	109.2702	28.0566	-78.999	47.70762	-102.882	174.1881	-97.9496	-136.249	-44.471	-261.534	506.5127	43.66704	-519.745	544.2185	-67.2001
ANN 9	82.83863	-16.6404	55.91193	-4.04999	-40.7518	47.41642	2.07614	30.50453	-17.4985	38.32662	-60.2273	9.254736	-2.8391	-161.247	32.50919	-49.9601	141.6616	38.4223	4.769415	36.60064	-48.7088	-44.9997
ANN 10	-6.85096	-15.5953	-53.8938	166.3463	-139.628	43.86689	-12.2645	293.9615	-94.796	-14.9778	174.4935	-357.057	67.30583	133.2397	-344.856	39.34847	77.74278	61.33149	-7.78001	-317.42	320.4425	-311.854
ANN 11	-4.14534	-280.541	77.32276	-178.979	354.8029	25.52599	-5.80604	112.0645	122.7073	-56.9441	-125.885	-39.5487	4.987985	541.8245	-116.352	135.0191	-368.752	-192.716	-299.634	156.5523	148.2754	144.7798
ANN 12	12.53011	-211.592	-64.7925	-2.98527	205.7329	67.17481	8.440962	318.0861	-296.172	418.4246	-329.206	-115.158	2.31991	-547.959	113.9723	-256.017	581.6414	106.9557	-111.226	-195.98	119.5278	188.8262
ANN 13	27.81297	111.9646	-184.873	89.30205	-23.9426	-4.05671	-6.68911	-932.331	160.0078	-153.013	586.3707	338.2248	-1.33566	-787.019	254.6646	-522.324	989.7836	66.79891	3.724917	-266.277	-275.299	264.1841
ANN 14	5.404288	-25.6471	-2.15878	27.49246	-25.68	27.87896	6.488907	-83.8165	10.78743	44.40674	-19.0553	51.36474	-12.2727	-53.9301	-6.79891	-16.8756	70.54426	0.451756	242.4743	-368.721	122.3573	-240.966
ANN 15	-1.32429	-339.074	61.24336	-123.313	348.1639	52.4126	1.341871	305.4	-3.05819	4.854538	-209.65	-93.9657	2.368872	-72.5248	-99.2085	129.4658	5.05473	14.68464	-305.982	207.3157	112.4547	98.73411
ANN 16	76.38504	-276.834	-191.783	195.6862	-45.0487	297.0826	15.6106	290.8855	-305.485	462.1689	-295.803	-149.869	0.079549	-126.054	190.0233	-434.492	569.1018	-189.918	-114.659	-135.941	122.1127	129.5649
ANN 17	0.638797	-112.699	38.76654	-73.0414	133.0714	14.5762	-0.38881	-28.8901	18.59899	-7.54966	-0.23067	18.64909	-1.64591	-31.9766	10.7093	-7.69066	15.32685	13.8652	-16.3358	24.88815	51.88782	-154.233
ANN 18	1.160381	123.679	-272.043	376.7367	-142.046	-89.4287	59.16837	13.32239	-347.584	119.0688	77.32606	106.2435	0.094556	93.72883	94.8292	-343.604	361.3542	-198.6	-14.6451	80.26411	-231.345	166.9035
ANN 19	25.13229	-69.8438	-155.084	21.04456	140.4304	48.98504	8.73015	218.1437	-185.984	260.9147	-190.979	-102.656	-2.67313	-25.358	-91.1295	294.1759	-269.293	92.71087	49.69896	-168.92	120.3051	-163.488
ANN 20	1.7777	49.01289	-16.3996	29.26337	-57.3003	-5.02118	-32.769	0.990202	-40.148	14.38911	14.61983	-13.6459	-0.79444	-23.8649	8.737991	-16.9147	31.70915	0.437318	-154.758	111.635	-21.6414	172.5172

C. "Shaded" classification ANNs

From:	bias	**R1-6**	**R7p**	**R7y**	**R8p**	**R8y**	bias	**R1-6**	**R7p**	**R7y**	**R8p**	**R8y**	bias	**R1-6**	**R7p**	**R7y**	**R8p**	**R8y**	bias	h1	h2	h3
To:	h1	h1	h1	h1	h1	h1	h2	h2	h2	h2	h2	h2	h3	h3	h3	h3	h3	h3	o	o	o	o
ANN 1	-34.6802	-4.21275	-4.17632	-5.36627	-5.47802	-2.56175	-14.5305	-8.48997	-7.77631	-8.07991	-8.90879	-7.03832	1.215478	23.39974	20.08521	21.9214	23.53257	25.54364	-49.5626	63.79984	28.59719	-81.049
ANN 2	-18.2326	56.27901	48.57529	50.86009	55.05732	59.80936	127.1638	230.457	214.1886	225.4053	232.9643	226.9184	-176.675	-21.9622	-31.5874	-33.0467	-28.4532	-4.40675	-238.171	-353.955	106.5588	283.2548
ANN 3	1.259232	14.92127	14.35867	13.80064	15.38755	16.49691	22.32186	6.997301	7.539857	7.633922	7.86974	7.438266	29.32325	3.306754	4.833231	4.108121	4.288051	2.340508	15.65593	-23.2155	-32.5253	-38.505
ANN 4	-94.4249	-13.8883	-14.6062	-16.914	-16.9	-5.77633	-3.38903	-7.96112	-6.46545	-7.8024	-7.75027	-8.00624	9.727399	-11.733	-10.0829	-10.561	-11.1973	-13.0391	-129.805	99.92419	3.502484	82.63009
ANN 5	-10.2689	-1.67331	-2.07178	-1.17929	-0.89566	-0.78028	-2.55706	-5.94842	-5.82087	-6.35693	-6.49616	-6.52033	-10.9738	-2.02503	-2.38762	1.903097	-0.36967	-3.98303	-33.7098	11.03626	17.49742	23.04077
ANN 6	57.4949	8.565758	6.673265	10.75126	11.87106	5.550123	5.431855	3.432265	1.633498	2.263986	3.248917	3.981596	-54.3373	-9.29724	-5.86892	-9.85395	-10.2211	-5.21554	-7.76299	-49.7961	-23.9199	56.98575
ANN 7	-36.5683	-6.13124	-5.93171	-7.08311	-7.63421	-4.09288	0.972395	-5.6062	-4.93296	-5.58228	-5.37277	-7.02403	32.60882	4.430099	5.859255	5.503251	5.72638	1.955724	-17.4414	60.85677	-12.314	-65.9831
ANN 8	-7.36974	-0.3439	-1.048	-1.42686	-1.20013	-0.07398	-138.536	-22.0271	-23.1608	-25.8413	-25.8792	-14.1476	21.32055	-0.04525	0.684507	0.685214	0.612835	-2.33156	-223.492	54.77454	191.5631	46.39096
ANN 9	60.63965	12.43292	-1.14988	3.248672	10.58831	14.79972	8.009288	15.03771	14.77921	15.35307	14.76646	15.2592	-6.53102	-10.8498	-8.49618	-9.34237	-10.1311	-11.4141	-65.8495	-155.283	23.23533	101.0613
ANN 10	-23.2047	-4.82944	-4.81726	-5.45478	-4.94567	-3.60738	-3.90347	10.5249	9.949209	9.311048	10.96742	11.90629	14.40437	1.006581	2.464949	1.798723	2.121799	1.138903	-19.7892	74.12368	-36.0102	-58.798
ANN 11	-82.7527	-21.5967	0.025683	-8.32074	-18.0024	-23.7771	-16.4232	5.242071	9.221842	6.378717	4.293844	4.69364	192.2957	31.0603	22.53821	32.60653	35.21408	19.1836	-44.3502	78.01278	-0.02061	-75.34
ANN 12	-18.2721	-2.3006	-3.72889	-2.79858	-1.61896	-1.93944	-15.2776	-7.05169	-7.04646	-7.31184	-7.77881	-7.18986	14.53141	5.811129	7.066686	7.481644	6.191565	3.150508	-52.4934	43.23089	25.40039	3.232401
ANN 13	-36.5085	4.770508	5.678982	4.912773	5.111673	6.152777	-61.4205	-12.001	-3.41206	0.634465	-6.88762	-17.4497	10.5016	1.986106	2.702762	1.484605	2.446513	1.677249	-26.0553	0.713841	55.01123	0.740771
ANN 14	29.37701	5.362204	1.895997	2.219075	5.496202	5.222522	2.903588	8.989776	8.593194	8.645981	9.03653	9.820774	20.66425	11.07529	7.750093	7.776673	10.32192	11.92051	15.21028	-36.351	-5.61221	-33.0992
ANN 15	-24.8837	-4.66157	-1.84289	0.478547	-2.47298	-6.53946	-25.884	-5.29767	-4.69704	-5.3851	-6.20758	-3.45472	19.40163	4.059966	2.27067	-2.00202	0.281537	8.31369	-4.57799	16.94904	2.738532	-15.4483
ANN 16	-22.4346	-3.27712	-2.29715	-4.06286	-4.29592	-1.61677	19.76979	5.002005	4.210742	4.911541	5.863722	4.3837	46.1611	6.153077	5.355873	5.921662	7.426246	3.707702	-4.78388	34.53668	-24.6179	-44.4021
ANN 17	26.4503	3.738638	3.821765	3.875756	4.698712	2.592881	13.00147	1.845204	2.184881	2.20454	1.847034	0.655286	8.836809	15.59595	15.07285	14.74357	15.96391	16.69354	27.57445	-37.3169	-33.7578	-11.2261
ANN 18	-57.346	-8.58239	-8.90198	-10.1881	-9.41687	-5.08955	4.451273	13.58398	11.95962	13.4194	13.49428	14.28077	17.98346	-28.5294	-24.9515	-25.5978	-26.8596	-31.1624	-32.4235	97.94673	-9.77572	-45.6872
ANN 19	-127.851	-23.3009	-2.2017	-11.6092	-22.6911	-20.8295	-11.7407	-22.9514	-19.8002	-21.3356	-23.1106	-22.1112	99.04361	-5.85352	-13.4364	-8.10655	-4.92332	-10.8281	-43.6111	143.5519	-11.2768	-58.3218
ANN 20	51.54802	7.188112	2.311039	6.534349	8.400401	5.677184	-1.22843	3.782162	2.881507	3.422595	4.128799	3.132471	-7.78739	-18.31	-16.4426	-17.0165	-18.0696	-18.1976	-1.90643	-54.6751	-25.6028	36.62211

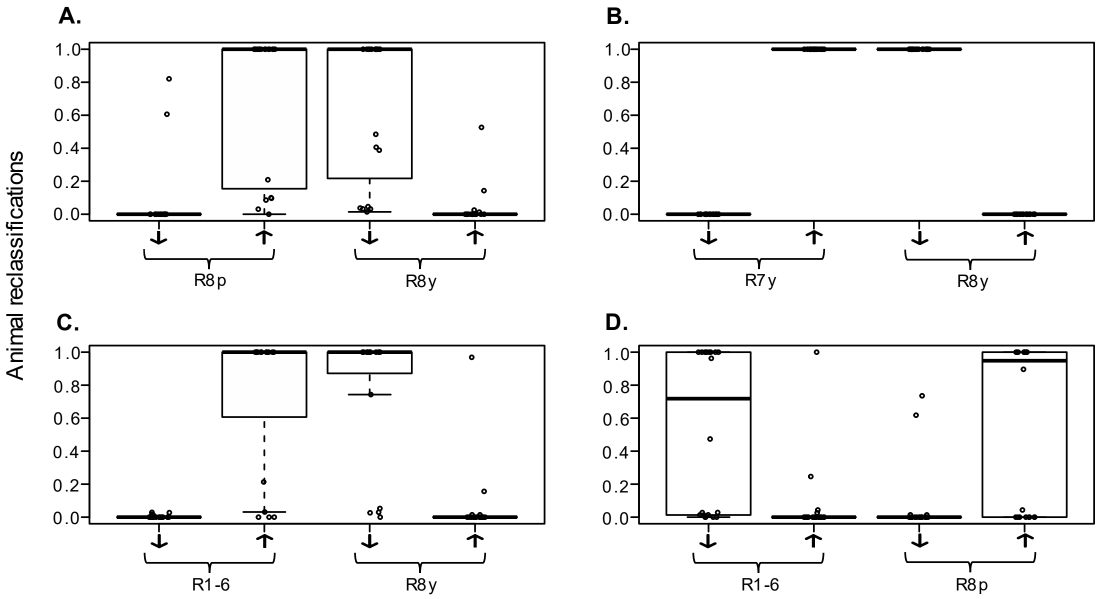

Figure S6. The contribution of photoreceptor excitation signals to animal-ANNs receiving two photoreceptor excitation inputs. Data are shown for the four two-photoreceptor-input animal-ANNs achieving best classification accuracy. The inputs to these were: (A) R8p and R8y, (B) R7y and R8y, (C) R1-6 and R8y, and (D) R1-6 and R8p. To produce these plots, one or other photoreceptor excitation input was clamped at its median value and those stimuli whose classification changed as a result of clamping were identified. The proportion of these reclassifications in which the classification changed from 'leaf' to 'animal' is shown, according to whether clamping increased or decreased the relevant photoreceptor excitation value for a given stimulus (indicated by an arrow). Models A-C have inputs from a blue-sensitive photoreceptor (R8p, R7y, or R1-6) and a green-sensitive photoreceptor (R8y). In all models, increases in the excitation of the photoreceptor with peak sensitivity at shorter wavelength (a blue-sensitive photoreceptor) are associated with stimuli being reclassified as animals, and decreases are associated with reclassification as leaves. Increases in the excitation of the photoreceptor with peak sensitivity at longer wavelength (the green-sensitive receptor in models for which it is involved) are associated with stimuli being reclassified as leaves, and decreases are associated with reclassification as animals. Plots show results for the best 20 ANNs of each type, superimposed over boxplots showing 25th, 50th and 75th percentiles.

C. Visualising principles of ANNs using a fly colour space

Here we report a graphical analysis of the stimuli analysed in our manuscript using a fly-specific colour space. Colour spaces can be constructed by removing luminance information from an n-dimensional receptor space to produce an n-1-dimensional colour space [8], but for a fly such a projection would have four dimensions. We use instead the only available colour space for flies based upon physiological information and behavioural results [9, 10]. This space is defined by comparison of the R7 and R8 photoreceptors found within a given ommatidium type, namely R7y-R8y and R7p-R8p. When considered in this colour space, the loci of leaf and animal stimuli overlap but separate best on the vertical axis, corresponding to a comparison of the green-sensitive R8y photoreceptor and the UV-blue-sensitive R7y photoreceptor (fig S7A). This corresponds to the various blue-green opponencies identified by our ANNs. Blue control devices are widely separated from the original stimulus clusters but are more extreme on this axis (black control devices occupy similar loci to the original cluster), corresponding with our conclusion that they activate the blue-green opponent mechanisms that would normally separate animals from leaves (fig S7A). Shaded and unshaded stimuli do not inhabit separate loci within this colour space. However, if the broadband R1-6 photoreceptor signal is used in place of the horizontal axis, shaded and unshaded stimuli are clearly separated (fig S7B). This aligns with the finding from our ANNs that shaded and unshaded stimuli can be separated based on achromatic information in the responses of single photoreceptors.

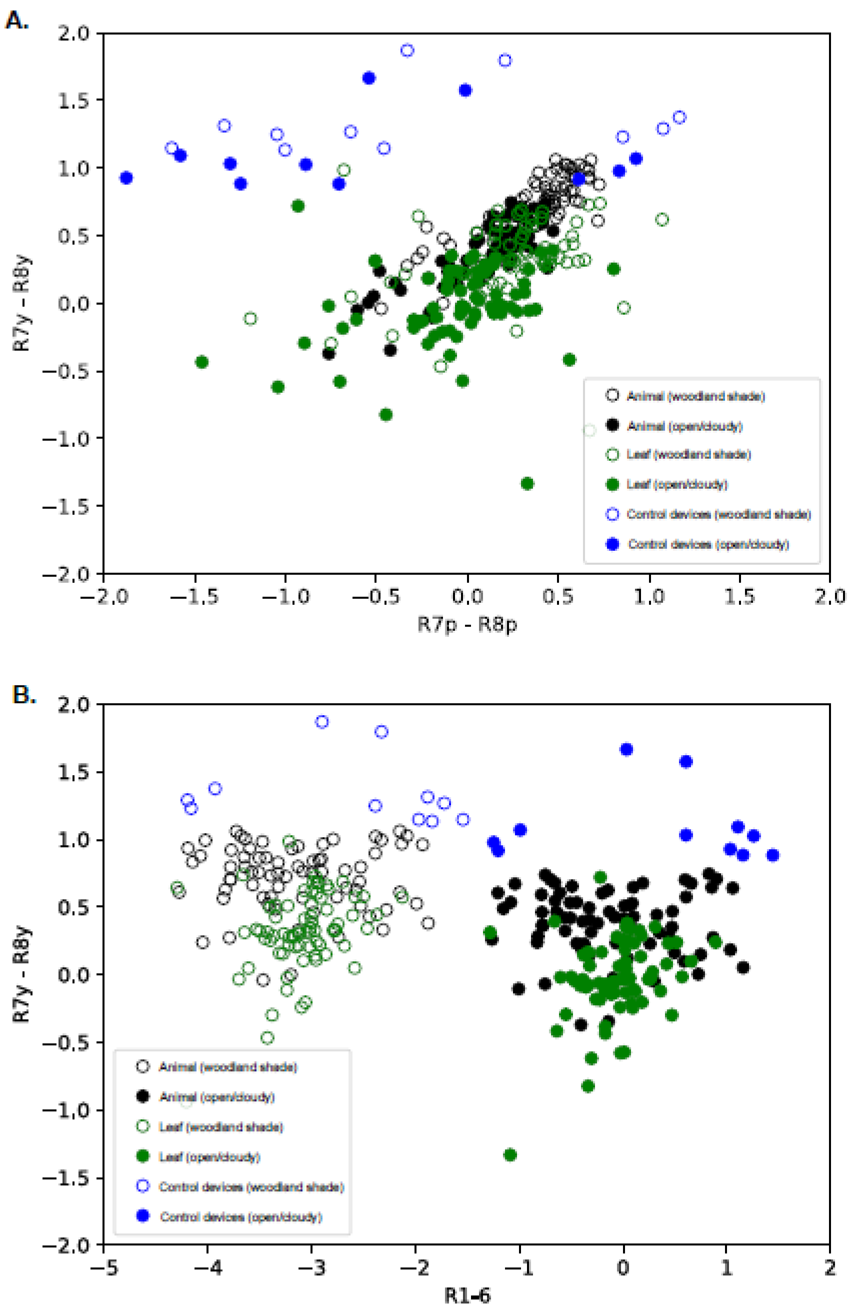

Figure S7. Stimuli represented in a fly colour space using photoreceptor excitation values as in our manuscript. (A) Animal and leaf stimuli inhabit similar loci within this space but are separated on the axis corresponding to a green vs UV-blue photoreceptor signal comparison (R7y – R8y). Blue (and other) control devices inhabit loci more extreme along this same axis. The three devices that appear furthest to the right comprise the black fabrics tested. (B) Shaded and unshaded stimuli could not be separated in part A, but can be separated using a single photoreceptor response (e.g. R1-6 shown here). These principles correspond with those identified by ANNs.

References

[1] Chittka, L. & Kevan, P.G. 2005 Flower colour as advertisement. In *Practical Pollination Biology* (eds. A. Dafni, P.G. Kevan & B.C. Husband), pp. 157-196. Cambridge, ON, Canada, Enviroquest Ltd.
[2] Hardie, R.C., Vogt, K. & Rudolph, A. 1989 The compound eye of the tsetse fly (*Glossina morsitans morsitans* and *Glossina palpalis palpalis*). *J. Insect Physiol.* **35**, 423-431.
[3] Santer, R.D. 2017 Developing photoreceptor-based models of visual attraction in riverine tsetse, for use in the engineering of more-attractive polyester fabrics for control devices. *PLoS Negl. Trop. Dis.* **11**, e0005448.
[4] Lindh, J.M., Goswami, P., Blackburn, R., Arnold, S.E.J., Vale, G.A., Lehane, M.J. & Torr, S.J. 2012 Optimizing the colour and fabric of targets for the control of the tsetse fly *Glossina fuscipes fuscipes*. *PLoS Negl. Trop. Dis.* **6**, e1661.
[5] Green, C.H. 1988 The effect of colour on trap- and screen-oriented responses in *Glossina palpalis palpalis* (Robineau-Desvoidy) (Diptera: Glossinidae). *Bull. Ent. Res.* **78**, 591-604.
[6] Green, C.H. & Flint, S. 1986 An analysis of colour effects in the performance of the F2 trap against *Glossina pallidipes* Austen and *G. morsitans morsitans* Westwood (Diptera: Glossinidae). *Bull. Ent. Res.* **76**, 409-418.
[7] Santer, R.D., Vale, G.A., Tsikire, D. & Torr, S.J. 2019 Optimising targets for tsetse control: Taking a fly's-eye-view to improve the colour of synthetic fabrics. *PLoS Negl. Trop. Dis.* **13**, e0007905.
[8] Kelber, A., Vorobyev, M. & Osorio, D. 2003 Animal colour vision - behavioural tests and physiological concepts. *Biol. Rev.* **78**, 81-118.
[9] Troje, N. 1993 Spectral categories in the learning behaviour of blowflies. *Z. Naturforsch.* **48**, 96-104.
[10] Lunau, K. 2014 Visual ecology of flies with particular reference to colour vision and colour preferences. *J. Comp. Physiol. A* **200**, 497-512.